Annals of Biomedical Engineering, Vol. 44, No. 4, April 2016 (© 2015) pp. 847–862
DOI: 10.1007/s10439-015-1521-2

Multi-Dimensional Nanostructures for Microfluidic Screening of Biomarkers: From Molecular Separation to Cancer Cell Detection

ELAINE NG,[1] KAINA CHEN,[2] ANNIE HANG,[2] ABEER SYED,[2] and JOHN X. J. ZHANG[2]

[1]Department of Bioengineering, Stanford University, Stanford, CA 94305, USA; and [2]Thayer School of Engineering, Dartmouth College, Hanover, NH 03755, USA

(*Received 30 October 2015; accepted 20 November 2015; published online 21 December 2015*)

Associate Editor Jennifer West oversaw the review of this article.

Abstract—Rapid screening of biomarkers, with high specificity and accuracy, is critical for many point-of-care diagnostics. Microfluidics, the use of microscale channels to manipulate small liquid samples and carry reactions in parallel, offers tremendous opportunities to address fundamental questions in biology and provide a fast growing set of clinical tools for medicine. Emerging multi-dimensional nanostructures, when coupled with microfluidics, enable effective and efficient screening with high specificity and sensitivity, both of which are important aspects of biological detection systems. In this review, we provide an overview of current research and technologies that utilize nanostructures to facilitate biological separation in microfluidic channels. Various important physical parameters and theoretical equations that characterize and govern flow in nanostructure-integrated microfluidic channels will be introduced and discussed. The application of multi-dimensional nanostructures, including nanoparticles, nanopillars, and nanoporous layers, integrated with microfluidic channels in molecular and cellular separation will also be reviewed. Finally, we will close with insights on the future of nanostructure-integrated microfluidic platforms and their role in biological and biomedical applications.

Keywords—Microfluidics, Nanostructures, Molecular separation, Cellular separation, Biomarkers, Passive separation, Point-of-care.

INTRODUCTION

Integration of microfluidics into analytical systems provides several advantages including, but not limited to, sample quantity reduction, shorter time-to-result, easy fabrication, lower cost, and high-throughput. Additionally, microfluidics embodies fundamental micro- and nanoscale physical phenomenon that enhances device performance. High surface-to-volume ratio leads to little or no diffusion which allows effective and efficient interfacial reactions, thus increasing the sensitivity of microfluidic platforms.[15] Conventional analytical tools for biology include mass spectrometry, liquid chromatography, and UV–vis spectrophotometry, all of which are disadvantaged in cost, size, sample preparation, sensitivity, or accuracy. As described by Lion *et al.*, performance of an analytical system can be impacted by two parameters, sample volume and time-to-result, making up what is termed "the analytical triangle". In comparing microfluidic immunoassays to microtiter plate immunoassays and protein microarrays, for the same level of performance, microfluidic immunoassays outperforms the other two, requiring less sample volume and shorter time-to-result.[49] Much research has been done to take conventional analytical methods and scaling them down to micro- and nanoscale regimes to improve performance, from centrifugal microfluidics[2,6,27,71] to electrophoretic microfluidics[18,36,66] to mass spectrometric microfluidics.[37,53,65] As a result of such advantages, microfluidics has been a tool of interest in a variety of biological applications, particularly in molecular and cellular separations and detection.

Given all the advantages that microfluidics provides in molecular and cellular separations, efforts are being made to improve performance of microfluidic devices. They include introduction of nanostructures as physical barriers to trap, filter, or size-select molecules and cells[21,56,58,69] and functionalized nanostructures to enhance sensitivity.[29,82] Nanostructures can be defined as structures with any one dimension between 1 and 100 nm.[3] Nanoparticles or quantum dots are zero-dimensional nanostructures, nanotubes, rods, and wires, or quantum wires, are one-dimensional nanostruc-

Address correspondence to Elaine Ng, Department of Bioengineering, Stanford University, Stanford, CA 94305, USA. Electronic mails: elaineng@stanford.edu and John.Zhang@dartmouth.edu

tures, and nanotextured surfaces or quantum wells are two-dimensional nanostructures.[76] In this review, we focus on recent developments in microfluidics that utilize nanostructures to facilitate biological molecular and cellular separations and detection. The integration of nanostructures into microfluidics for biological applications is a prime example of powerful point-of-care devices that effectively increase performance while decreasing time-to-result and sample volume (see Fig. 1). Here, we review the integration of nanoparticles and nanomagnets, pillars and rods, and micro- and nanoscale mesoporous films in microfluidic channels for both molecular and cellular separation. We will discuss the physical advantages that nanostructures contribute to microfluidic-based molecular and cellular separations. In each section, we will highlight specific examples of microfluidic systems that incorporate nanostructures to enhance molecular or cellular separation. We briefly summarize the method of fabrication and then highlight the characteristics that define the structure. In addition, we will present the structure in the context of its biological motivation and how it achieves biological separation, providing a comparison of the nanotechnology described with other conventional technologies that have been developed with the same functionality, if available. Finally, we will conclude with an overview of the future of nanostructure-integrated microfluidic systems as potential practical and viable biomedical solutions to a variety of patient healthcare needs, including those of diagnostic and therapeutic values.

WHY NANOSTRUCTURES IN MICROFLUIDICS?

Microfluidics is the use of small channels with dimensions on the order of tens to hundreds of microns to manipulate small volumes of fluids.[80] At microscale, the fluid flow is associated with negligible inertia and gravity whereas capillary forces are surface tension dominated.[62] Microfluidics contributes several advantages in as biological analytical systems, as previously

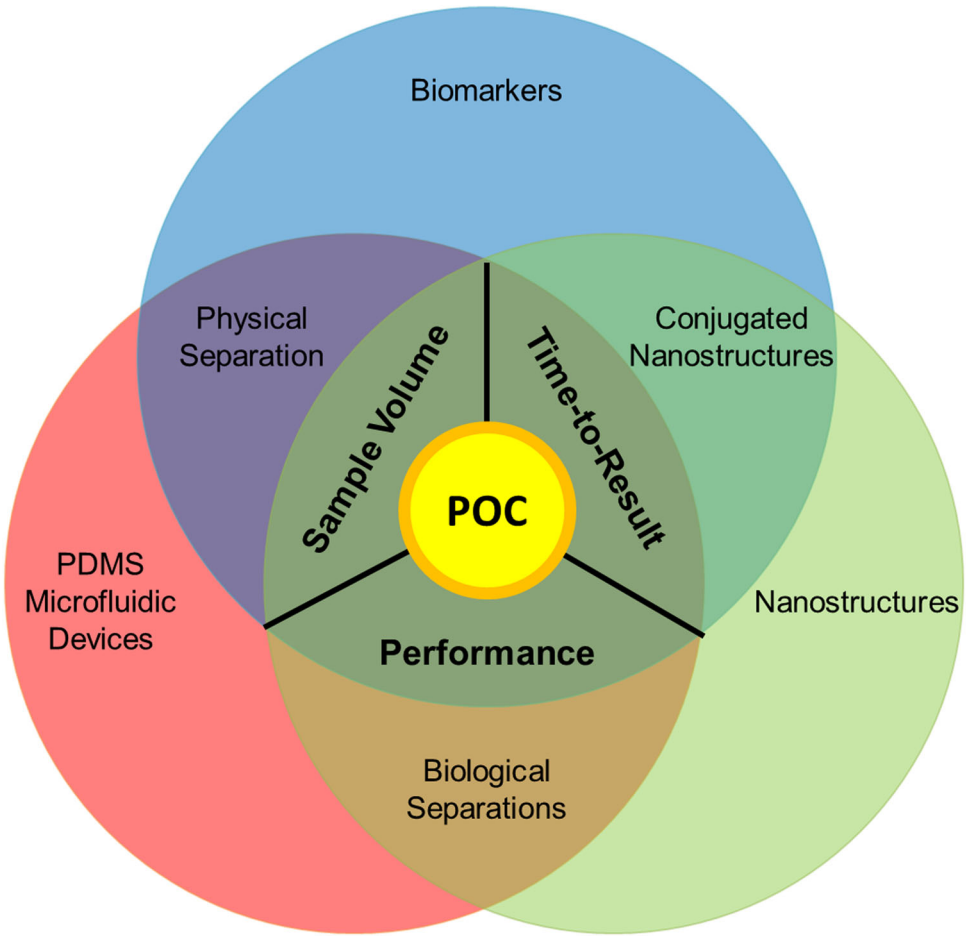

FIGURE 1. Point-of-Care biomarker detection using nanostructure-integrated microfluidic devices. Various analytical techniques have been developed to compete in terms of performance, sample volume and time-to-result. Nanostructures, coupled with microfluidics, have been successful in performing biological and physical separations at both molecular and cellular scale.

mentioned. Microfluidic devices are already capable of providing a platform for continuous hydrodynamic-driven size-based filtration of cells,[13,25,86,87] and molecular separation including, but not limited to, protein [38,47,57] and DNA [41,42,78] separations and detection. So what more would the integration of nanostructures into microfluidic channels provide? By introducing nanostructures into microfluidic systems, we can broaden the range of applications available for microfluidic manipulations and improve upon current microfluidic systems.

Figure 2a represents most flows in microfluidic systems where Reynolds number ($Re = \frac{\rho UL}{\eta}$, where ρ is density, U is velocity, L is length of the channel, and η is shear viscosity), a dimensionless parameter that describes the ratio of inertial and viscous forces, is assumed to be low ($\mathrm{Re} \ll 1$)[17] and the flow of an incompressible fluid through a microchannel is laminar and is described by Navier–Stokes equation $(\rho(\frac{\partial u}{\partial t}) + u\nabla u = -\nabla p + \mu\nabla 2u + f$, where u is fluid velocity field, f is vector field of the external forces acting on the fluid, and p is pressure field).[17,68]

The Péclet number, another dimensionless parameter described by $Pe = \frac{UL}{D}$ (where U = velocity, L = length of the channel, and D = diffusivity) determines whether the mass transport is dominated by diffusion or convection. If $\mathrm{Pe} > 1$, then diffusion dominates and if $\mathrm{Pe} < 1$, convection dominates. The flow in microfluidic channels have a typically large, providing flow conditions whereby mixing is essentially non-existent,[68] thus decreasing the sensitivity of the microfluidic device as molecules and cells may never physically make contact with the capture surface.

Integrated nanostructures in microfluidic channels introduce turbulence into the flow, resulting in decreased mixing times and shorter mixing distances, effectively increasing mixing in the microchannel (Fig. 2b). Depending on the particular application, especially in sensing systems, this advantage increases sensitivity of the device by increasing the interfacial surface area (Figs. 2c and 2d). In addition, adding nanostructures to microfluidic channels increase overall interfacial surface area which can also increase sensitivity of devices by providing more places for analyte and sensor interactions. Nanostructures provide physical barriers making intricate size-dependent separations of particles of more than two sizes possible (Fig. 2f)[30] in comparison with simple microfluidic de-

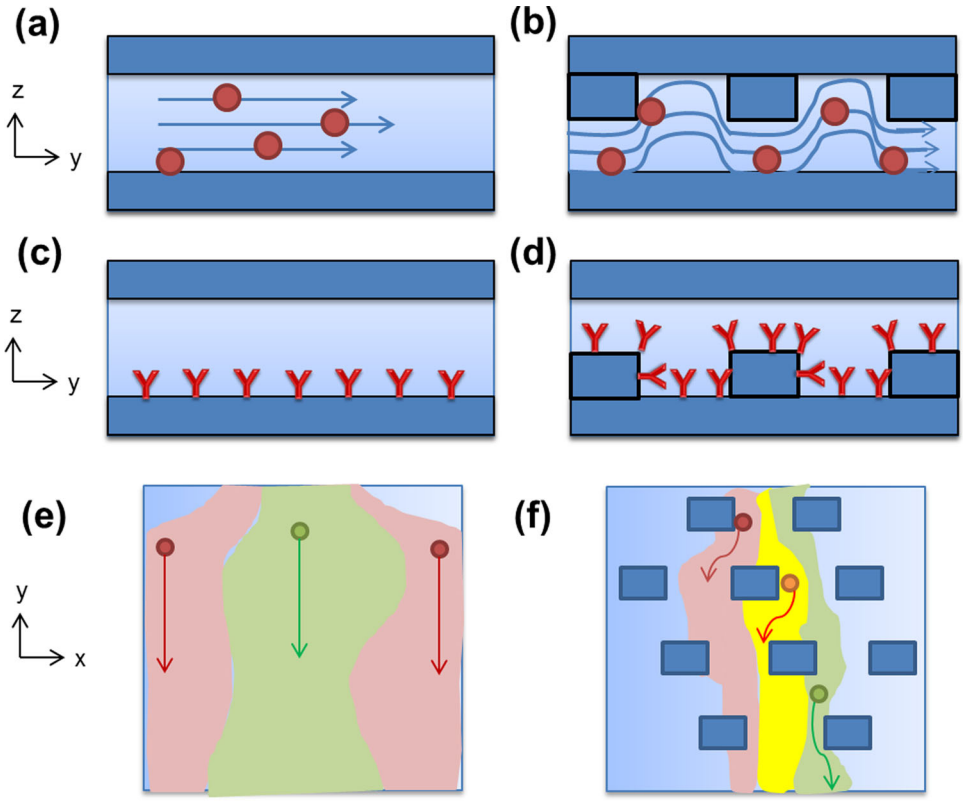

FIGURE 2. Nanostructures facilitate molecular and cellular separation and detection. Nanostructures can (a) introduce turbulent and micromixing environments that increase analyte-surface interactions, (b) increase interfacial surface area available for sensing elements, and (c) enable higher order separation capabilities. These additional advantages can increase specificity, sensitivity, efficiency, and effectiveness of the microfluidic system.

vices which are limited to the separation of only two different sized particles and specificity may be relatively lower (Fig. 2e).[13,25,86,87]

SEPARATION WITH ZERO-DIMENSIONAL NANOSTRUCTURES: NANOPARTICLES

Nanoparticles are small beads ranging from 1 to 100 nm in diameter.[12,40] Nanoparticles show a wide range of physical and optical properties due to their quantum-scale dimensions.[1] They can be mass produced and surface-conjugated.[50] Iron oxide nanoparticles have magnetic properties, colloidal gold nanoparticles have unique optical light-scattering properties, and tagged fluorescent polystyrene beads can simplify visual identification. The versatility of nanoparticles makes them prime candidates in facilitating molecular and cellular separations.

Nanoparticles for Molecular Separations

Magnetic iron oxide nanoparticles have a unique applicability in molecular separations. The nanoparticle surface can be coated with specific antibodies,[14,19,77] nucleotides,[7,55,73] peptides,[26,46,83] or other molecules[44,48,88] that attract the object of interest (Fig. 3).

In a microfluidic channel, the magnetic properties of these particles allow the nanoparticles and target molecules to be physically manipulated using electromagnetics or permanent magnets.[40] Malhotra *et al.*, developed a gold nanoparticle (AuNP) immunoarray in a microfluidic channel to measure interleukin 6 (IL-6), interleukin 8 (IL-8), vascular endothelial growth factor (VEGF) and VEFG-C simultaneously in diluted serum for sensitive oral cancer detection. The device had eight sensor elements and used streptavidin coated magnetic beads labelled with enzymes and secondary antibodies to bind the proteins. Once the analyte proteins were bound to magnetic beads, the beads were washed and passed through the array for selective capture of proteins with an 89 and 98% sensitivity and specificity, respectively.[52] Kim *et al.* demonstrated the magnetic force based immunoassay using superparamagnetic 50 nm nanoparticles and 1 μm fluorescent polystyrene beads. The NeutrAvidin coated polystyrene beads were used to immobilize biotin conjugated anti-rabbit and anti-mouse IgG. The antibody-labeled superparamagnetic nanoparticles were used as labels of sandwich immunoassay. When the target analyte is added to the mixture, it interacts simultaneously with the microbeads and magnetic particles. The superparamagnetic particles bind to the microbeads by antigen–antibody complex. Under the influence of applied magnetic field in a microchannel, only the beads that have attached to the magnetic particles move to the higher gradient magnetic field. The magnetic force (F_{sm}) acting on the microbeads and the velocity (V) of the microbeads in the solution can be calculated using the following equations respectively: $F_{sm} = \frac{V_{sm}\Delta\chi_{sm}}{2\mu_0 \cdot \nabla B^2}$, $V = \frac{N_{sm}V_{sm}\Delta\chi_{sm}}{12\pi R_M \eta \mu_0 \cdot \backslash \mathrm{n}\nabla \mathrm{B}^2}$, where V_{sm} is volume of superparamagnetic particles, $\Delta\chi_{sm}$ is net magnetic susceptibility of a superparamagnetic particle in aqueous solution, N_{sm} is number of the superparamagnetic beads attached to the microbead, μ_0 is vacuum permeability, B is magnetic field, R_M is radius of microbead, and η is viscosity of the aqueous medium.[40] Another commonly used nanoparticle in biological separations is gold nanoparticles. Luo *et al.* discusses

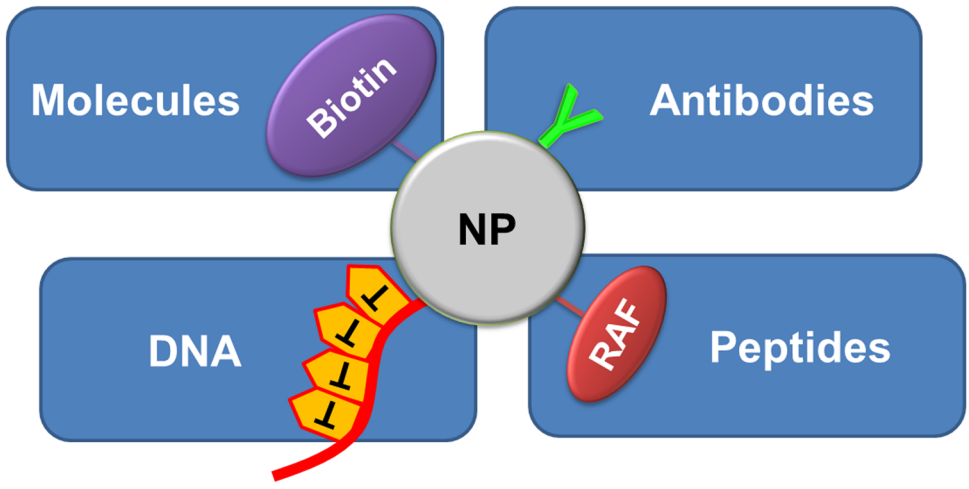

FIGURE 3. Schematic representation of most commonly used functionalized nanoparticles for biological applications. Nanoparticles display a wide range of physical, chemical, and biological functionalities due to their versatile and tunable properties and characteristics. Most importantly, nanoparticle surfaces can be functionalized with various moieties, such as antibodies, nucleotides, peptides, and other molecules for targeted separations.

an aggregate-based immunoassay system for goat anti-human IgG protein detection. Gold nanoparticles, coated with goat anti-human IgG protein antigen, were deposited on a microfluidic channel to capture the antibodies flowing through the system. After tuning parameters such as flow velocity and reaction time, detection of concentrations as low as 10 ng/mL was found to be possible.[51] Gold nanoparticles have also been used to improve the resolution of molecular separation in capillary electrophoresis. The microfluidic channels were coated with a layer of PDADMAC (poly(diallyldimethylammonium chloride). The high charge-density property of the PDADMAC allows the gold nanoparticles to be adsorbed on the channels walls altering the inner topography of the microfluidic channel and reverses the electroosmotic flow resulting in improving the electrochemical detection twofold.[59]

Lai *et al.* exploited dual magnetic and temperature responsive nanoparticles to facilitate capture of diagnostic analytes. Carboxylate-terminated telechelic poly(N-isopropylacrylamide) polymer chains (PNIPAAm) were attached to the surface of superparamagnetic nanoparticles. These polymer chains are temperature responsive, can be easily conjugated with proteins of interest, and exhibit a low critical solution temperature (LCST) at which they aggregate into hydrophilic stimuli-responsive micelles. When integrated into polyethylene glycol (PEG)-ylated microfluidic channels at a temperature below the LCST of the polymer chains, the magnetic nanoparticles are soluble and flow through the channel, capturing target molecules. When the temperature is raised above the LCST and a magnetic field is applied, flow conditions change and the nanoparticles aggregate on the channel walls, separating captured molecules from the channel's flow stream. This process is also reversible. When the magnetic field is removed and temperature lowered, nanoparticles in solution regain their mobility and are eluted out with bound molecules. These responsive nanoparticles can facilitate controlled molecular separation through simple manipulation of physical conditions.[43]

As previous examples illustrated, incorporation of nanostructures in microfluidic channels can aid in the miniaturization of whole laboratory procedures. To demonstrate an example of lab-on-chip, Chen *et al.* implemented a three-step process of bead mixing, magnetic separation and viral protein concentration and elution in the same device. The bead-mixing step consists of mixing the viral lysate sample with the immunomagnetic nanoparticles. High-gradient magnetic concentrators (HGMC) were used to concentrate the magnetic field for improved magnetic separation. HGMC takes advantage of uneven and angular magnetic materials that exhibit higher localized magnetic fields, which in this case are randomly close-packed polydisperse iron particles (25–75 μm in diameter). Furthermore, close packing of the particles within a tiny channel volume ensure proximity between nanoparticles and capture surface, enhancing separation efficiency. Additional herringbone structures generate a micromixing environment, maximizing interaction between particles and viral sample. Magnetic separation is therefore achieved by immunomagnetic assay of viral proteins, followed by elution of separated proteins for downstream quantification and analysis. This separation system results in a significantly heightened concentration (40–80 fold increase) of HIV viral protein from human plasma in twenty minutes.[8]

Nanoparticles for Cellular Separations

Nanoparticles are an efficient and powerful way to isolate rare cells from complex heterogeneous samples, such as blood. As previously mentioned, the high surface to volume ratio enables high density functionalization for effective contact with cell surfaces and the small size minimizes aggregation of particles. In comparison to conventional micron-sized particles, nanoparticle-based cellular separation results in less aggregation, less damage to cells, higher mobility, stronger binding ability, and higher stability.[85] Magnetic nanoparticles can be conjugated with antibodies to from an immunomagnetic label. Superparamagnetic iron oxide nanoparticles are more commonly used in cellular separations, mostly due to its high magnetic saturation, biocompatibility, and ability for its surface to be chemically modified to attach biological 3 moieties.[22,45] Such particles can be conjugated with specific antibodies that bind respectively to unique surface antigens on the cell of interest, enhancing specificity and sensitivity of targeted cellular separation in microfluidic-based immunomagnetic assays (Fig. 4).

Xu *et al.* demonstrated the power of using nanoparticles in an immunomagnetic assay for human epithelial growth factor receptor 2 (HER2) positive SkBr3 breast cancer cells. From a 1 mL spiked blood sample with 0.05 mL of nanoparticles, they were able to perform a microfluidic-based immunomagnetic assay with capture rates of 76.3%, which represents a 23.5% improvement over the use of microparticles.[85] Another interesting application of nanoparticles in microfluidic devices was demonstrated by Xia *et al.* A microfabricated high gradient magnetic field concentrator (HGMC) was placed on one side of the microfluidic channel, and upon magnetization, nanoparticles functionalized against *Escherichia coli* (*E. coli*) bacteria were pulled from the initial flow stream and into a collection stream. This device

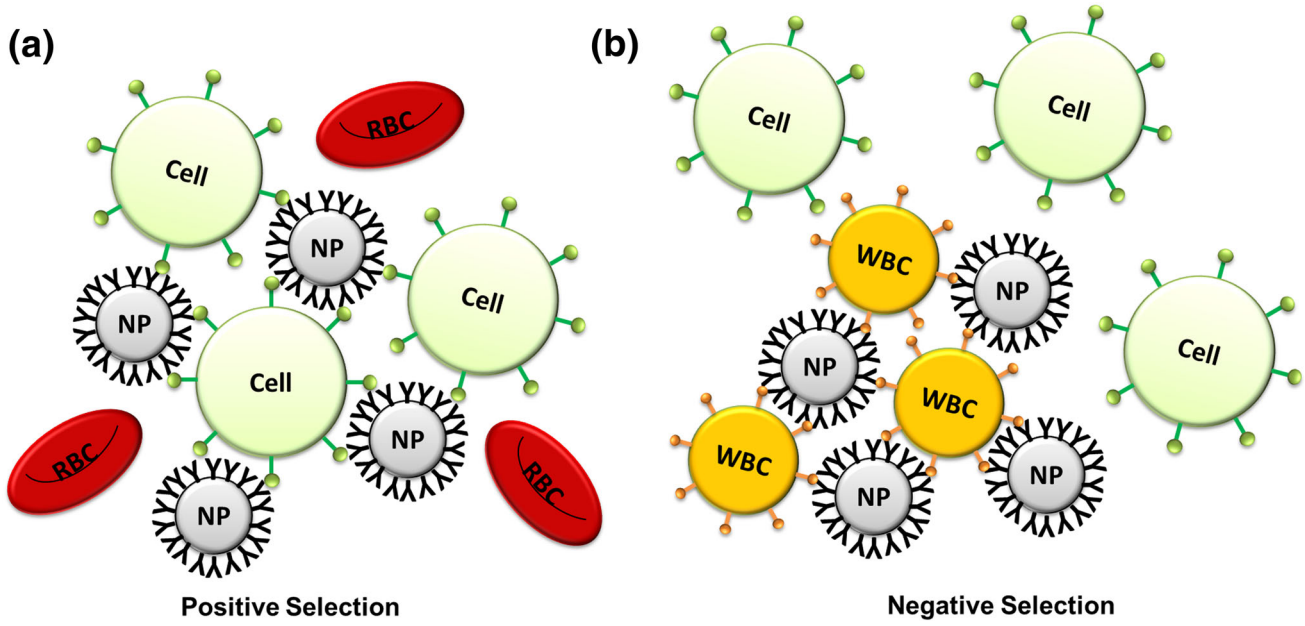

FIGURE 4. Schematic of immunomagnetic positive and negative enrichment of CTCs. (a) In positive enrichment, magnetic nanoparticles labeled with anti-CTC antibodies (e.g., anti-EpCAM or anti-HER2) are incubated with whole blood, and bind to antigens present on the surface of the CTCs. As the mixture passes through the magnetic field, CTCs are positively selected and retained while the rest of the blood cells are eluted out. (b) In negative enrichment, other cells are labeled with nanoparticles and retained while CTCs are eluted out.

allowed continuous separation of living *E. coli* from solutions containing red blood cells (RBCs). It was reported that almost all (89%) *E. coli* were pulled into the lower flow path from a solution of low RBC concentration. It was observed that due to increased viscosity at physiological concentrations of RBCs, separation efficiency experienced a decrease to 53%, which only improved to 78% upon doubling the ratio of magnetic nanoparticles to *E. coli*.[84]

Recent research has placed much emphasis on early cancer detection through the detection of circulating tumor cells (CTCs). CTCs are tumor cells that have detached from primary tumor sites and circulate in the peripheral circulatory system or lymphatic system.[54] As they circulate, some become lodged at secondary organ sites where they remain dormant until triggered by specific cellular signals, wherein they begin the process of metastasis, growing and developing into a secondary cancerous tumor site. It is this metastatic process that makes cancer such a difficult disease to fight. Hence early detection and diagnostics has become a hot topic of research in efforts for early prevention. Micro- and nanoscale systems provide an attractive approach to cellular separations with increased sensitivities and specificities.[5,60]

Huang *et al.* designed a practical and interesting method of CTC detection using magnetic nanoparticles in microfluidic devices. They were able to capture CTCs from SkBr3, PC3, and Colo205 cell lines by labeling them with anti-EpCAM functionalized Fe_3O_4 nanoparticles and passing them through a motion controlled microfluidic-based immunomagnetic system. A PDMS microchannel is bonded to a glass slide and three rectangular permanent magnets are attached to the other side. An automatic rotational microchip holder holding more than one microchip highly parallelizes the system and orients the microfluidic chips in an optimal position, inverting them to counterbalance the effects of gravitational sedimentation and decreasing non-specific settling of RBCs on the glass slide (Fig. 5a). As the blood sample flows through the channel, the magnets attract nanoparticles that are attached to CTCs bringing the nanoparticle-CTC complex to the glass surface while the rest of the sample flows into a waste reservoir. To minimize clogging and nanoparticle aggregation, a spacer was placed between the first half of each magnet and the glass slide to minimize the magnetic flux density at the beginning of the channel (Fig. 5b). Labeled CTCs flow towards the stronger magnetic field at the second half of the channel and avoiding nanoparticle aggregation at the front end of the channel. Fluorescence staining of separated and captured CTCs can then be used for identification. For spiked samples, the microchip performed with an average capture rate of 97, 107, and 94% for SkBr3, PC3, and Colo205, respectively.[31]

A novel modification of the aforementioned microchip was the incorporation of a patterned Cr/Ni

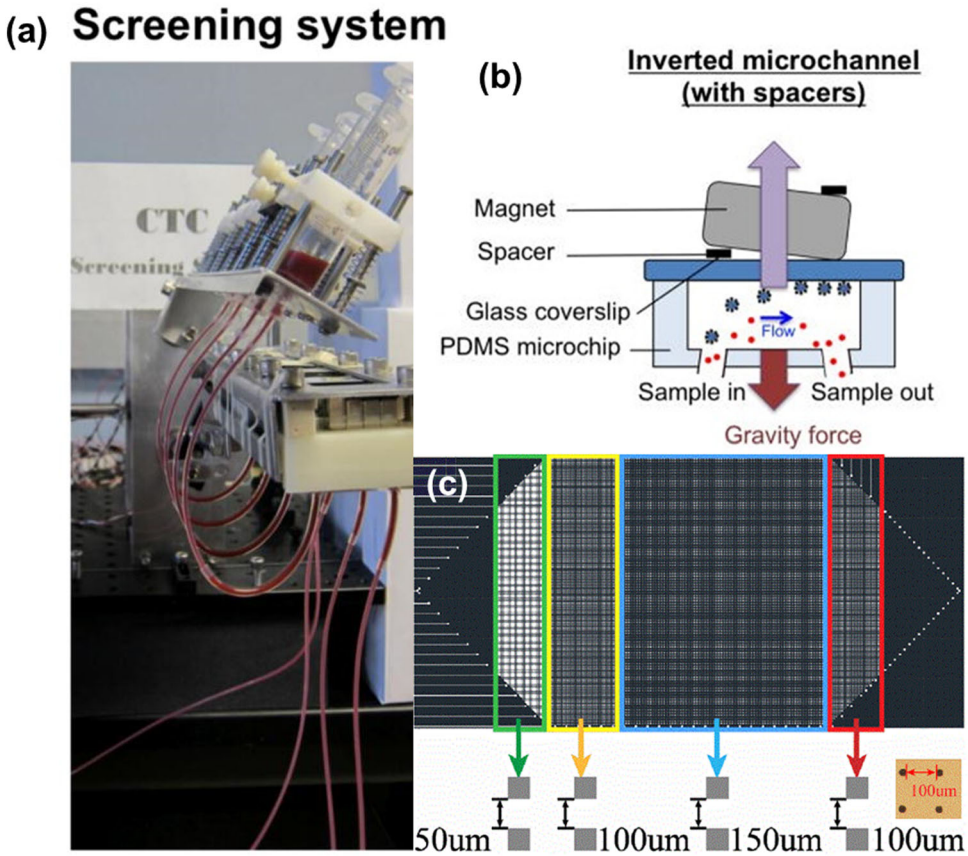

FIGURE 5. Nanoparticles and nanomagnets for cellular separation. (a) Highly parallelized microfluidic chip inverting system designed to minimize non-specific gravitational sedimentation of RBCs during CTC capture and separation. (b) Spacers generate a magnetic field gradient that increases throughout the microchannel, thus minimizing clogging. Figures adapted from Ref. 31. (c) Addition of nanomagnet arrays on the capture glass slide at varying densities enhances localized magnetic fields, leading to a more uniform distribution of the field and again reduces nanoparticle aggregation. Figure adapted from Ref. 9.

metal nanomagnet array on the glass slide (Fig. 5c).[32] When the permanent magnet is the sole source of magnetic field, the largely uneven distribution of the magnetic field causes the aggregation of nanoparticles, causing 90% of the cells to be captured at the front edge of the permanent magnet.[9] This poses a problem because the dense aggregation of nanoparticles and cells in one place may damage fragile CTCs during the separation process. Incorporating nanomagnets reduces this complication by generating gentle local magnetic fields. A single nanomagnet increases the local field intensity by 8 times.[32] With the integration of nanomagnets into the microfluidic channel, the nanoparticles' adherence pattern disperses and the channel usage increases by 23%. In addition, the nanomagnets decreased the degree of nanoparticle aggregation by 20%, suggesting that this system reduces the amount of excess nanoparticles which could hinder analysis.[9] It is noted that the nanomagnets must be thin as to limit collision and consequent damage to the CTCs in the microfluidic channel.[10]

SEPARATION WITH ONE-DIMENSIONAL NANOSTRUCTURES: NANOPILLARS

Nanopillars are one-dimensional nanostructures that work effectively as molecular separators by disrupting hydrodynamic flow profiles of molecules within microfluidic channels. This manipulation can be used to separate molecules based on different physical or chemical properties. Thus, nanopillar-integrated microfluidic systems also provide an attractive alternative to current molecular and cellular separation techniques.

Nanopillars for Molecular Separations

Manipulation of nanopillar geometries allows size-dependent separations possible. Shi *et al.* fabricated a parallel nanopillar array composed of two nanopillar arrays with same periodicity but different feature sizes, one being 300 nm and the other being 200 nm. Integrated with a microfluidic channel, they demonstrated

separation of 48 kbp λ DNA and 166 kbp T4 DNA, both displaying different stretching effects. Both DNA fragments stretched in the 300 nm nanopillar array. However, T4 DNA, because of its larger size, stretched significantly more than λ DNA. In the 200 nm array, T4 DNA was stretched, while λ DNA remained spherical.[64] The geometry and arrangement of nanopillars is critical for molecular separation. Huang *et al.* demonstrated this by using an array of obstacles that are carefully placed based on geometric parameters such as obstacle periodicity, $\frac{\Delta\lambda}{\lambda} = \frac{1}{3}$, where $\lambda = 8\ \mu$m is the center-to-center distance between obstacles, and gap distance, $d = 1.6\ \mu$m. With this design, they made use of asymmetric bifurcation of laminar flow around obstacles, separating microspheres of three different sizes (0.80, 0.90, 1.03 μm diameter).[30]

By manipulating nanopillar arrangements between a tilted array and a square array, Yasui *et al.* were able to separate DNA molecules based on near-equilibrium and non-equilibrium transport. In the square array pattern, adjacent nanopillars are arranged parallel to the flow stream whereas in the tilted array pattern, nanopillars are staggered such that they are inclined 45° to the flow stream.[89] In equilibrium transport, DNA molecules are separated due to physical interactions between structures and DNA molecules, as in conventional electrophoresis and chromatography. In the tilted nanopillar array, a significant tradeoff between separation speed and resolution was observed. By designing a square nanopillar array, non-equilibrium transport was used to separate different sized DNA molecules at faster times and maintained separation resolution. The nanopillars 500 nm in diameter and 4000 nm in height were fabricated on quartz substrate using electron beam lithography, electroplating, and etching, and spaced 300–1000 nm apart. It was found that larger molecules migrated faster than smaller molecules. This observation can be explained by the rotational Péclet (Pe_r) number, which is directly proportional to the torque induced by the electric field. The Pe_r number is given by the following equation: $Pe_r = \frac{M}{k_B T} = \left(\frac{1-\delta}{1+\delta}\right)\left(\frac{\hat{q}E_{av}L^2}{k_B T}\right)$, where $k_B T$ is Boltzmann factor, M is electric-field-induced torque, δ is spacing ratio, $\hat{q}$ is DNA charge per unit length, E_{av} is averaged electric field, and L is contour length of the DNA molecule. Thus, a molecule under high electric fields that crosses the threshold Pe_r, will transit from diffusion-based transport to non-equilibrium transport. Larger DNA molecules, when placed under a non-uniform electric field gradient, occupy a wider area of the gradient than the smaller molecule and therefore experience a stronger torque that causes them to align along the electric field. This alignment enables rapid transit through the microchannel without interference with nanopillars, whereas smaller molecules that are poorly aligned with the electric field experience more physical interactions with the pillars (Fig. 6a). Using this square nanopillar array, Yasui *et al.* was able to separate four different sized DNA molecules at good resolutions within 60 s.[90]

Another interesting use of nanopillars is the ciliated micro/nano fluidic device used for selectively trapping exosome like lipid vesicles (Wang *et al.*, Fig. 6b). Exosomes are lipid membrane vesicles that are shed from viable cells and contain a variety of biological content such as lipids, proteins, and RNA that provide

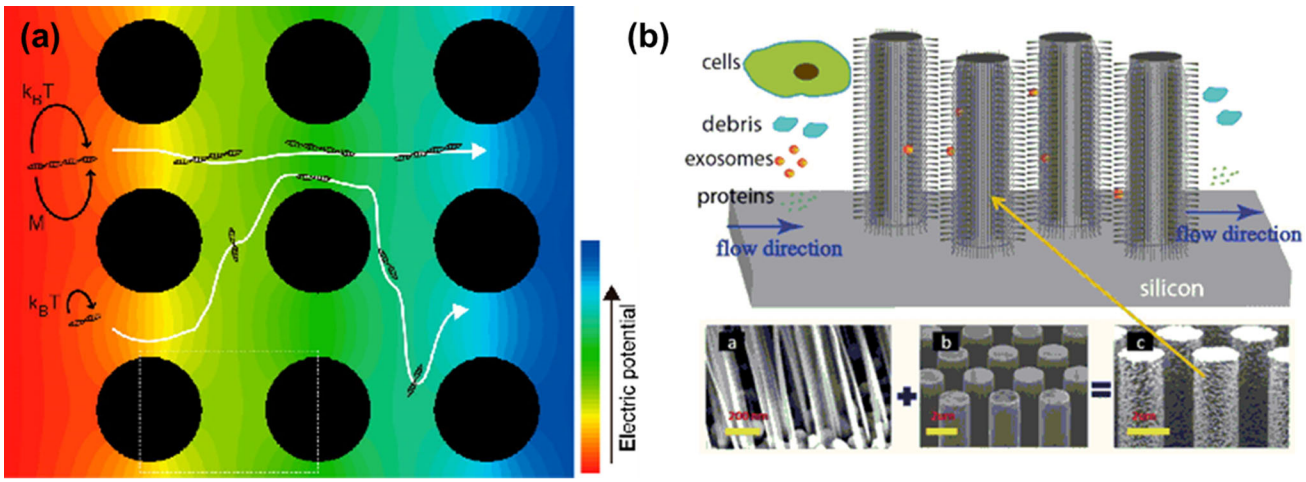

FIGURE 6. Nanopillars for molecular separation. (a) Square array of nanopillars effectively separate DNA molecules of various sizes in a non-uniform electric field gradient. Larger DNA fragments experience a stronger torque that aligns them along the electric field, enabling a straight projection through the array. Figure adapted from Ref. 90. (b) Ciliated micropillars enable molecular separation on a multitude of levels, separating cells, debris, and proteins from desired exosomes. Figure adapted from Ref. 79.

information on the cells and tissues from which they originated.[75] Conventional exosome isolation is performed using differential centrifugation which results in inconsistent recovery rates and lower purity.[74] The ciliated nanoporous nanowire-on-micropillar structures were fabricated using microfabrication, electroplating, and electroless metal-assisted nanowire etching. The nanowires are spaced 30–200 nm apart, creating dense forests for trapping exosome-like particles. The micropillars block cells and the nanowire forest blocks submicron debris, letting proteins pass through. Only exosome-sized objects are trapped in interstitial spaces within the nanowire forest, which can then be dissolved in phosphate buffered saline for recovery. The efficiency of this device is about 60% for the 83 nm liposomes used to mimic exosomes in 30 μL sample volume, a significantly higher retention rate compared to the conventional differential centrifugation method (5–23%).[79]

Nanopillars for Cellular Separations

As previously mentioned, nanopillars provide additional advantages in enhancing sensitivity of microfluidic-based separation devices. By optimizing nanopillar geometries and placement, sensitivity can be increased by maximizing cell-to-pillar interactions. This was shown by Nagarth *et al.* in what has been coined the "CTC-chip". The CTC-chip was designed based on two parameters: (1) flow velocity, which influences cell-pillar contact duration, and (2) shear force, which influences cell-post attachment. Using computational simulations of cell-post interactions and cell flow path, the CTC-chip was designed using optimal parameters of a 50 μm separation between posts and a 50 μm shift after every 3 rows. The chip consists of a total of 78,000 posts. Capture efficiencies were consistently about 65% when assaying samples with cell lines of varying EpCAM expression and with spiked cells in blood samples. Nagarth *et al.* also performed CTC separation with their CTC-chip using clinical samples from patients with non-small cell lung cancer (NSCLC), prostate, pancreatic, breast, and colon cancers. From these experiments, they reported 99.1% sensitivity and 100% specificity across all five cancers with high reproducibility. Another major advantage the CTC-chip provides is the elimination of blood sample pre-processing. As such, the CTC-chip provides a good illustration of how nanostructures aid microfluidic cellular separations and enable them to become a clinically useful and powerful tool.

Similar to nanopillars, another two-dimensional structure has been shown to aid in CTC capture and separation. First coined by Stott *et al.* as the "Herringbone (HB)-Chip", this chip integrated HB structures, or surface ridges, with microfluidics to create a microvortexing, or micromixing, environment. In such an environment, the HB structures serve to disrupt the laminar flow streamlines characteristic of microchannels, thus introducing turbulence in flow that maximizes collisions between target cells and the capture surface, which in this case are EpCAM coated walls. The HB-chip was designed with geometries that optimized the ratio of height of the grooves to that of the channel, chevron dimensions, and periodicity for cellular separation. The chip was simply constructed by bonding a glass slide to a PDMS structure consisting of eight microchannels with HB structures patterned on the upper surface. Stott *et al.* compared capture efficiencies of the HB-Chip with those of a flat-wall chip. It was found that the HB-Chip had high capture efficiencies at low flow rates (about 79%) and was able to maintain high capture efficiencies at higher flow rates ($>40\%$) whereas the flat-wall chip only had 29% capture efficiencies at lower flow rates which dropped significantly to $<8\%$ at high flow rates. Capture efficiencies for prostate cancer PC3-spiked clinical samples were as high as 91%, and out-performed the aforementioned CTC-Chip in purity by 5%. With the HB-Chip, Stott *et al.* demonstrated to ability to perform post-capture and separation analysis of cells, including viability assays, *in vitro* culturing, and fluorescence *in situ* hybridization (FISH). Actual clinical patient samples at various stages of treatment for prostate and lung cancer were processed on the HB-Chip, where the detection threshold for significance was determined to be $\geq$10 CTC/mL. With the captured cells, they were able to perform post-capture analysis of patient samples using reverse transcription polymerase chain reaction (RT-PCR), as well as immunofluorescence staining for on chip cellular identification. Again, the HB-Chip, like its predecessor, the CTC-Chip, utilizes nanostructures to greatly enhance cellular separation and capture in microfluidic devices. In addition, this second generation chip improves upon some of the drawbacks of the CTC-Chip, leading to a more robust and analyzable system, allowing for large scale production and chemical modifications, and the ability to image captured cells in a transparent channel.[69] These modifications demonstrate a place for such nanostructure-integrated microfluidic chips in clinical point-of-care technologies.

SEPARATION WITH TWO-DIMENSIONAL NANOSTRUCTURES: MESOPOROUS FILMS

Physical properties of mesoporous films provide a variety of advantages which have been utilized in

biological molecular separations[20,28,33,35,39,57] and size-based filtration of molecular species.[21,70] Current size-based molecular separation involves gel-based techniques such as gel electrophoresis or gel-filtration (size-exclusion) chromatography for DNA, RNA, or protein separation. However, resolutions of gel-based techniques are not ideal and usually require pH modifications of the gels to increase resolution, but at the expense of small dynamic ranges. In addition, sample extraction after separation is difficult.[61] Mesoporous films can be fabricated with self-assembling techniques that allow for control of pore sizes, which in turn provide increased separation resolutions.[34,35]

Mesoporous Films for Molecular Separations

Desai *et al.* previously demonstrated fabrication of micromachined silicon membranes with pore sizes of 25.4 nm using a combination of photolithography and deposition and selective removal of sacrificial layers, to perform separation of glucose.[16] Striemer *et al.* demonstrated fabrication of ultrathin membranes about 10 nm thick with pore sizes in which they varied from 5 to 25 nm. By simply controlling thermal annealing temperatures during crystallization, they were able to control the nanocrystal nucleation and growth and hence the pore size of the silicon membrane. The design of membranes with varying pore sizes allows for size-based filtering of biological macromolecules, in this case, the separation two common proteins in biological samples, bovine serum albumin (BSA) and immunoglobulin G (IgG) antibodies.[70] Sharma *et al.* employed the use of mesoporous silica in a unique application, separating glucose and oxygen molecules for use in ultra-thin implantable glucose biofuel cells.[63]

The coupling of nanopore or nanofilter structures with microfluidics allows effective sample extraction after separation for downstream analysis, as demonstrated by Fu *et al.* By introducing continuous flow using microfluidics, steady harvesting of biological molecules can be possible, essentially constructing a microscale dialysis system. A molecular sieving microfluidic system was fabricated using photolithography and reactive ion etching (RIE, Fig. 7b). This "anisotropic nanofilter array" (ANA) is capable of performing continuous-flow separation of DNA and proteins *via* various sieving mechanisms, such as Ogsten sieving, entropic trapping, or electrostatic sieving, thus allowing separation of a complex biological sample containing molecules of broad dynamic range of sizes, charge, and molecular properties. By simply changing buffer ionic strengths, separation of DNA fragments and proteins of varying sizes under two independent electric fields, E_x and E_y, can be achieved.

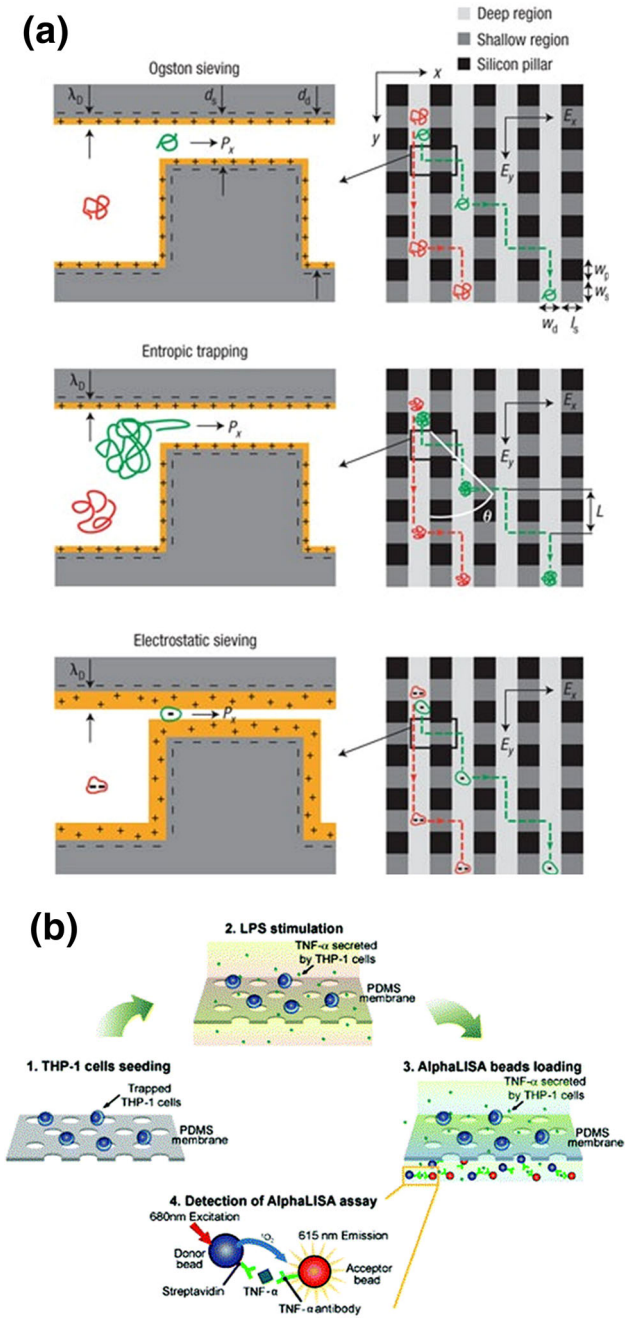

FIGURE 7. Nanofilters and mesoporous structures for molecular separation. (a) Nanofilters consisting of an array of shallow and deep channels, termed nanosieves, can effectively perform size-dependent and electrostatic separation of DNA and proteins *via* Ogsten sieving, entropic trapping, or electrostatic sieving. Figure adapted from Ref. 21. (b) Micropores make up a microfiltration membrane that effectively separates cells from secreted cytokines, enabling effective and efficient secretome detection. Figure adapted from Ref. 29.

For small molecules in high ionic strength buffers, the Debye length, λ_D (Fig. 7a), is negligible relative to depth of the nanofilters, d_s.[21] The Debye length is given

by the following equation: $\lambda_D = \left(\frac{\varepsilon_0 \kappa_B T}{n_0 e^2}\right)^{\frac{1}{2}}$, where ε_0 is permittivity of free space, k_B is Boltzmann constant, T is temperature, n_0 is electron density, and e^2 is electron charge.[23] In this case, Ogsten sieving occurs whereby smaller molecules travel a shorter mean characteristic drift distance, L, in the deep channels with a larger stream deflection angle, θ. For larger molecules with diameters greater than the nanofilter constriction size, steric hindrance is the limiting factor and entropic trapping occurs whereby longer molecules travel a shorter L with a larger θ. In low ionic strength buffers, $\lambda_D \approx d_s$ and molecules with lower net charge travel a shorter L with a larger θ. Separation speed and resolution can be controlled by modulating the two independent electric fields. Fu and Schoch *et al.* were able to separate small DNA fragments ranging from 150 to 1000 bp with Ogsten sieving and large DNA fragments ranging from 2000 to 23,130 bp with entropic sieving. They also demonstrated separation of three different proteins, lectin, fibrogen, and B-phycoerythrin. One potential limitation of this system though is the need for careful choice of experimental conditions. The three aforementioned proteins were effectively separated in Tris–borate-EDTA (TBE) 5 × buffer under $E_x = 100$ V cm^{-1} and $E_y = 50$ V cm^{-1}. However, because lectin and streptavidin have similar molecular weights, the two proteins were indistinguishable in TBE 5×, but by lowering the ionic strength of TBE to 0.05×, the two proteins separated due to differences in isoelectric points.[21]

Recent developments also focus on integrating nanostructures in microfluidic channels to create lab-on-chip devices, as demonstrated by Huang *et al.* who developed a microfluidic platform that performs immune cell seeding, cell stimulation, and cell-secreted cytokine immunoassay on a single chip (Fig. 7b). Microfluidic channels are used to seed initial cells and to deliver necessary reagents, media, and nutrients to maintain and culture cells. Upon stimulation, the immune cells secrete tumor necrosis factor-α (TNF-α), a cytokine, which is filtered and separated from cells by a polydimethylsiloxane (PDMS) microfiltration membrane (PMM). TNF-α can then be detected and quantified using AlphaLISA, a no-wash, photo-induced chemiluminescence, bead-based sandwich ELISA technique. In this device, the PMM is critical allowing the separation and enrichment of TNF-α from the immune cells. The PMM is an effective filtration area of 7 mm^2 with thickness of 10 μm consisting of 4 μm pores, fabricated using contact photolithography and reactive ion etching. More importantly, the efficiency of separation and cytokine diffusion is dependent on membrane porosity, which was optimized to a high porosity of 25% for this particular application. This device well-illustrates the advantage of using micro- and nanoporous structures in molecular separation, enabling rapid real-time analyte detection as well as higher analyte retention.[29]

Mesoporous Films for Cellular Separations

Mesoporous films provide physical structures that increase roughness and surface area of substrate surfaces, allowing size-selective trapping of proteins and enhance protein adsorption.[4,57] Blinka *et al.* previously showed that nanoporous silica thin film functionalized substrates enhance protein adsorption onto substrate surfaces more so that surfaces chemically functionalized by 3-aminopropyltriethoxysilane (APTES) and glutaraldehyde (GA). It was also found that nanoporous silica substrates characterized by 4 nm pores, 30–100 nm thin film thickness, and 57% porosity were most effective in protein adsorption.[4]

Nanoporous silica thin films with such characteristics, especially 4 nm pore sizes, assist in anchoring IgG antibodies, with typical dimensions of 8.5 nm × 14.4 nm × 4 nm,[67] in place on substrates, optimally exposing epitopes for antigen binding. This effectively lends itself to use in separation and detection of proteins *via* antibody-antigen interactions in biological assays such as sandwich enzyme-linked immunosorbent assays (ELISAs). ELISAs are based on the complementary binding between analyte of interest with corresponding labeled antibodies specific to the analyte of interest. The label on the detection antibody generates a physical signal that indicates the presence of the analyte of interest and can be further processed to determine quantitative information.[24] Conventionally, ELISAs are performed in microtiter plates, utilizing sample and reagent volumes ranging from 100 to 300 μL. Additionally, ELISA testing requires long procedures, about 10 h long. By using microfluidics, sample and reagent volumes can be reduced by about fivefold to a few microliters and time-to-result can be reduced to time scale of minutes.[49]

However, given the advantages of the microfluidic channel, much of the immunoassay quality is dependent on its starting piece, the capture antibody and how well it is anchored to the substrate surface. Without effective functionalization of the capture antibody onto the substrate surface, the sensitivity of the ELISA would be reduced. Hence, nanoporous silica thin films provide an effective working platform for ELISAs. Ng *et al.* previously used the microcontact printing technique, a protein transfer technique for producing self-assembled monolayers (SAMs),[81] to physically transfer a uniform monolayer of capture antibodies onto nanoporous silica substrates and demonstrated a system for performing multiplexed

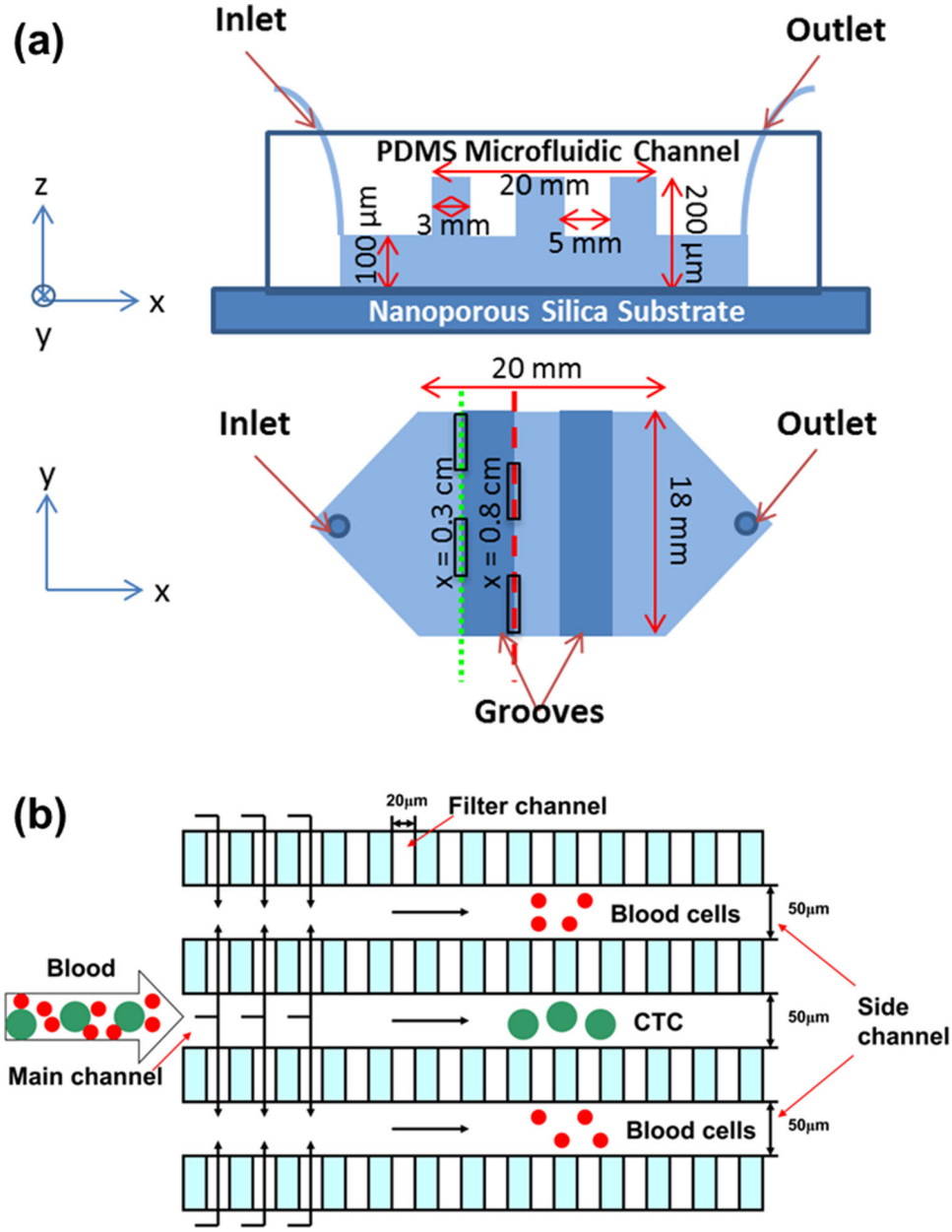

FIGURE 8. Nanofilters and nanoporous films for cellular separation. (a) Side and top view of grooved microchannel design. Optimal (green dotted lines) and non-optimal (red dotted lines) locations for cell-surface interactions are shown. Black boxes indicate areas of patterned anti-EpCAM antibodies. Main sample microchannels are separated from side microchannels by nanofilter channels. Figure adapted from Ref. 58. (b) Main microchannels are separated from side channels by nanofilter channels that effectively separate CTCs from other cellular components in blood. Figure adapted from Ref. 72.

ELISAs for protein separation and detection.[57] Nanoporous silica film substrates were fabricated through self-assembly of surfactant micelles by polymer units mixed with soluble silicates, tetraethyl orthosilicate (TEOS) and tetraethoxysilane, in homogenous, hydro-alcoholic solutions. During spin coating, the solvent evaporates, increasing polymer concentration and when exceeding critical micelle concentration, drives silica/co-polymer self-assembly into a uniform thin film phase. Furthermore, Ng *et al*. integrated patterned nanoporous silica substrates with grooved microfluidic channels to perform targeted site-specific cell separation, capture, and detection (Fig. 8a). As previously mentioned the porous nature of mesoporous films increases the surface area of the substrate and therefore increases the capture antibody density per unit area, which in turn, increases the sensitivity of the ELISA system, an important advantage in biological

detection, especially in rare cell detection. Uniquely, by patterning the nanoporous silica substrate and integrating it with a grooved microchannel, they were able to dictate optimal and non-optimal sites for cell capture. Epithelial cell adhesion molecule (EpCAM) positive SkBr3 breast and Colo205 colon cancer cell lines were captured in patterned optimal areas vs. in non-stamped areas.[58] The integration of patterned nanoporous silica substrates with microfluidic channels enables effective and efficient cell separation and capture.

In addition to enhanced protein adsorption to aid in ELISA detection systems, mesoporous films aid in the physical trapping and partitioning of cells by taking advantage of the biomechanical properties of cells themselves. Chen *et al.* demonstrated the separation of CTCs based on differential adhesion preference of CTCs for nanoroughened surfaces. Using reactive ion etching and photolithography, they were able to spatially pattern nanoroughened surfaces, and therefore capture CTCs in cellular mixtures with around 88–95% capture efficiency. These yields were better compared to the capture yields on smooth glass surfaces (14–22%). This goes to show that based on differential mechanical properties, CTCs can be separated from other cell populations through use of nanostructures.[11]

Incorporation of microfluidics with porous structures enables efficient and effective filtering systems that rely on differences between cell sizes and deformability between CTCs and other blood cells. Such a filtration system was demonstrated by Sun *et al.* who fabricated a simple multichannel microfluidic chip characterized by 50 μm high main and side channels separated by filter channels of 5 μm in height (Fig. 8b). Fabrication of the chip simply involved multilayer soft lithography of a PDMS microfluidic piece that was then bonded to a glass slide. As sample enters the main channels, pressure difference between the main and side channel cause small-sized blood cells to be filtered out into side channels through the filter channels and eliminated at the waste chamber, whereas larger cells such as CTCs remain in the main channel. Interestingly, upon comparison with typical EpCAM-based immunomagnetic separation, the microfluidic filtration device outperformed with above 80% recovery rates at various cell concentrations, compared to the inconsistent lower recovery rates (36–81%) obtained through immunomagnetic separation. In addition, when functionalized with EpCAM capture antibodies, the microfluidic filtration device did not show significant enhancement of recovery rate. However, it is also important to note that since the device is size-based, specificity of the captured CTCs must still be visualized with fluorescence microscopy. Sun *et al.* also proceeded to perform CTC capture and separation from rectal cancer patient blood samples, and with the microfluidic filtration device, as able to detect CTCs with counts above 3 CTCs per 5 mL blood. Furthermore, they were able to demonstrate the predictive power of the device, grouping patients into categories and stages (healthy, stage II–III, local recurrence, and metastasis) dictated by the range of captured CTCs. This is an illustrative example of how nanofilters are capable of enhancing microfluidic separations with clinical relevancy.[72]

CONCLUSION

Nanostructures play a significant role in enhancing microfluidic-based molecular and cellular separations. Ensuring effective and efficient separations of biological samples are critical in determining the sensitivity and specificity of the biomarker screening process, and especially when searching for low abundance analytes amongst a sea of complex mixtures. Nanostructures and the associated unique properties in physical, chemical and biological applications at small scales enable efficient manipulation of biological samples in microfluidic channels. In this review, we discussed three representative multi-dimensional nanostructures and how they were used to enhance protein adsorption, cancer cell screening and molecule filtration through modulation of the local environment. All these enhancements lead to enrichment of the analyte of interest for downstream analysis.

We illustrate the power of integrating functional multi-dimensional nanostructures into a single microfluidic system to perform biomarker screening with enhanced specificity. This forms the backbone of the complete lab-on-chip operations, from sample collection to analyte enrichment to post-separation detection and analysis. Such all-in-one nano-enabled microfluidic systems are key to the future direction of point-of-care diagnostics for global healthcare.

ACKNOWLEDGMENTS

The research is partially sponsored by National Institute of Health (NIH) National Cancer Institute (NCI) Cancer Diagnosis Program under grant 1R01CA139070. We would like to gratefully thank the National Science Foundation Graduate Research Fellowship (Elaine Ng) and the Dartmouth Women in Science Programs scholarship (Kaina Chen, Annie Hang) for the generous support.

REFERENCES

[1]Alivisatos, A. P. Semiconductor clusters, nanocrystals, and quantum dots. *Science (80-)* 271:933–937, 1996.

[2]Arosio, P., T. Müller, L. Mahadevan, and T. P. J. Knowles. Density-gradient-free microfluidic centrifugation for analytical and preparative separation of nanoparticles. *Nano Lett*. 14:2365–2371, 2014.

[3]Bhushan, B. Springer Handbook of Nanotechnology. Springer, 2010. https://books.google.com/books?hl=en&lr=&id=me1grr_pobMC&pgis=1.

[4]Blinka, E., K. Loeffler, Y. Hu, A. Gopal, K. Hoshino, K. Lin, X. Liu, M. Ferrari, and J. X. J. Zhang. Enhanced microcontact printing of proteins on nanoporous silica surface. *Nanotechnology* 21:415302, 2010.

[5]Bohunicky, B., and S. A. Mousa. Biosensors: the new wave in cancer diagnosis. *Nanotechnol. Sci. Appl*. 4:1–10, 2010.

[6]Burger, R., P. Reith, G. Kijanka, V. Akujobi, P. Abgrall, and J. Ducrée. Array-based capture, distribution, counting and multiplexed assaying of beads on a centrifugal microfluidic platform. *Lab Chip* 12:1289–1295, 2012.

[7]Cao, Y. C., R. Jin, and C. A. Mirkin. Nanoparticles with Raman spectroscopic fingerprints for DNA and RNA detection. *Science* 297:1536–1540, 2002.

[8]Chen, G. D., C. J. Alberts, W. Rodriguez, and M. Toner. Concentration and purification of human immunodeficiency virus type 1 virions by microfluidic separation of superparamagnetic nanoparticles. *Anal. Chem*. 82:723–728, 2010.

[9]Chen, P., Y.-Y. Huang, K. Hoshino, and X. Zhang. On-chip magnetic field modulation for distributed immunomagnetic detection of circulating tumor cells. *Solid-State Sens*. 2013. doi:10.1109/Transducers.2013.6626989.

[10]Chen, P., Y.-Y. Huang, K. Hoshino, and J. X. J. Zhang. Microscale magnetic field modulation for enhanced capture and distribution of rare circulating tumor cells. *Sci. Rep*. 5:8745, 2015.

[11]Chen, W., S. Weng, F. Zhang, S. Allen, X. Li, L. Bao, R. H. W. Lam, J. A. Macoska, S. D. Merajver, and J. Fu. Nanoroughened surfaces for efficient capture of circulating tumor cells without using capture antibodies. *ACS Nano* 7:566–575, 2013.

[12]Chikkaveeraiah, B. V., V. Mani, V. Patel, J. S. Gutkind, and J. F. Rusling. Microfluidic electrochemical immunoarray for ultrasensitive detection of two cancer biomarker proteins in serum. *Biosens. Bioelectron*. 26:4477–4483, 2011.

[13]Cho, B. S., T. G. Schuster, X. Zhu, D. Chang, G. D. Smith, and S. Takayama. Passively driven integrated microfluidic system for separation of motile sperm. *Anal. Chem*. 75:1671–1675, 2003.

[14]Day, E. S., L. R. Bickford, J. H. Slater, N. S. Riggall, R. A. Drezek, and J. L. West. Antibody-conjugated gold-gold sulfide nanoparticles as multifunctional agents for imaging and therapy of breast cancer. *Int. J. Nanomed*. 5:445–454, 2010.

[15]Delamarche, E., D. Juncker, and H. Schmid. Microfluidics for processing surfaces and miniaturizing biological assays. *Adv. Mater*. 17:2911–2933, 2005.

[16]Desai, T. A., D. J. Hansford, L. Leoni, M. Essenpreis, and M. Ferrari. Nanoporous anti-fouling silicon membranes for biosensor applications. *Biosens. Bioelectron*. 15:453–462, 2000.

[17]Di Carlo, D. Inertial microfluidics. *Lab Chip* 9:3038–3046, 2009.

[18]Duncombe, T. A., and A. E. Herr. Photopatterned free-standing polyacrylamide gels for microfluidic protein electrophoresis. *Lab Chip* 13:2115–2123, 2013.

[19]Eck, W., G. Craig, A. Sigdel, G. Ritter, L. J. Old, L. Tang, M. F. Brennan, P. J. Allen, and M. D. Mason. PEGylated gold nanoparticles conjugated to monoclonal F19 antibodies as targeted labeling agents for human pancreatic carcinoma tissue. *ACS Nano* 2:2263–2272, 2008.

[20]Feng, P., X. Bu, and D. J. Pine. Control of pore sizes in mesoporous silica templated by liquid crystals in block copolymer–cosurfactant–water systems. *Langmuir* 16:5304–5310, 2000.

[21]Fu, J., R. B. Schoch, A. L. Stevens, S. R. Tannenbaum, and J. Han. A patterned anisotropic nanofluidic sieving structure for continuous-flow separation of DNA and proteins. *Nat. Nanotechnol*. 2:121–128, 2007.

[22]Gupta, A. K., and M. Gupta. Synthesis and surface engineering of iron oxide nanoparticles for biomedical applications. *Biomaterials* 26:3995–4021, 2005.

[23]Haas, F. Quantum Plasmas. New York: Springer, 2011.

[24]Hornbeck, P. Enzyme-linked immunosorbent assays. *Curr. Protoc. Immunol*. Chapter 2: Unit 2.1, 2001.

[25]Horsman, K. M., S. L. R. Barker, J. P. Ferrance, K. A. Forrest, K. A. Koen, and J. P. Landers. Separation of sperm and epithelial cells in a microfabricated device: potential application to forensic analysis of sexual assault evidence. *Anal. Chem*. 77:742–749, 2005.

[26]Hosta-Rigau, L., I. Olmedo, J. Arbiol, L. J. Cruz, M. J. Kogan, and F. Albericio. Multifunctionalized gold nanoparticles with peptides targeted to gastrin-releasing peptide receptor of a tumor cell line. *Bioconjug. Chem*. 21:1070–1078, 2010.

[27]Hou, H. W., M. E. Warkiani, B. L. Khoo, Z. R. Li, R. A. Soo, D. S.-W. Tan, W.-T. Lim, J. Han, A. A. S. Bhagat, and C. T. Lim. Isolation and retrieval of circulating tumor cells using centrifugal forces. *Sci. Rep*. 3:1259, 2013.

[28]Hu, Y., A. Bouamrani, E. Tasciotti, L. Li, X. Liu, and M. Ferrari. Tailoring of the nanotexture of mesoporous silica films and their functionalized derivatives for selectively harvesting low molecular weight protein. *ACS Nano* 4:439–451, 2010.

[29]Huang, N.-T., W. Chen, B.-R. Oh, T. T. Cornell, T. P. Shanley, J. Fu, and K. Kurabayashi. An integrated microfluidic platform for in situ cellular cytokine secretion immunophenotyping. *Lab Chip* 12:4093–4101, 2012.

[30]Huang, L. R., E. C. Cox, R. H. Austin, and J. C. Sturm. Continuous particle separation through deterministic lateral displacement. *Science* 304:987–990, 2004.

[31]Huang, Y., K. Hoshino, P. Chen, C. Wu, N. Lane, M. Huebschman, H. Liu, K. Sokolov, J. W. Uhr, E. P. Frenkel, and J. X. J. Zhang. Immunomagnetic nanoscreening of circulating tumor cells with a motion controlled microfluidic system. *Biomed. Microdevices* 15:673–681, 2013.

[32]Huang, Y. Y., P. Chen, K. Hoshino, C. H. Wu, N. Lane, M. Huebschman, J. Uhr, K. Sokolov, E. Frenkel, and X. Zhang. Patterned nanomagnets on-chip for screening circulating tumor cells in blood. MicroTAS, 2012.

[33]Innocenzi, P., and L. Malfatti. Mesoporous thin films: properties and applications. *Chem. Soc. Rev*. 42:4198–4216, 2013.

[34]Innocenzi, P., L. Malfatti, and G. J. A. A. Soler-Illia. Hierarchical mesoporous films: from self-assembly to porosity with different length scales. *Chem. Mater*. 23:2501–2509, 2011.

[35]Innocenzi, P., Y. L. Zub, and V. G. Kessler. Sol-Gel Methods for Materials Processing. Dordrecht: Springer, 2008. doi:10.1007/978-1-4020-8514-7.
[36]Jha, S. K., R. Chand, D. Han, Y.-C. Jang, G.-S. Ra, J. S. Kim, B.-H. Nahm, and Y.-S. Kim. An integrated PCR microfluidic chip incorporating aseptic electrochemical cell lysis and capillary electrophoresis amperometric DNA detection for rapid and quantitative genetic analysis. *Lab Chip* 12:4455–4464, 2012.
[37]Ji, J., L. Nie, L. Qiao, Y. Li, L. Guo, B. Liu, P. Yang, and H. H. Girault. Proteolysis in microfluidic droplets: an approach to interface protein separation and peptide mass spectrometry. *Lab Chip* 12:2625–2629, 2012.
[38]Kamholz, A. E., B. H. Weigl, B. A. Finlayson, and P. Yager. Quantitative analysis of molecular interaction in a microfluidic channel: the T-sensor. *Anal. Chem.* 71:5340–5347, 1999.
[39]Kim, M., and T. Kim. Integration of nanoporous membranes into microfluidic devices: electrokinetic bio-sample pre-concentration. *Analyst* 138:6007–6015, 2013.
[40]Kim, K. S., and J.-K. Park. Magnetic force-based multiplexed immunoassay using superparamagnetic nanoparticles in microfluidic channel. *Lab Chip* 5:657–664, 2005.
[41]Lagally, E. T., I. Medintz, and R. A. Mathies. Single-molecule DNA amplification and analysis in an integrated microfluidic device. *Anal. Chem.* 73:565–570, 2001.
[42]Lagally, E. T., P. C. Simpson, and R. A. Mathies. Monolithic integrated microfluidic DNA amplification and capillary electrophoresis analysis system. *Sens. Actuators B Chem.* 63:138–146, 2000.
[43]Lai, J. J., J. M. Hoffman, M. Ebara, A. S. Hoffman, C. Estournès, A. Wattiaux, and P. S. Stayton. Dual magnetic-/temperature-responsive nanoparticles for microfluidic separations and assays. *Langmuir* 23:7385–7391, 2007.
[44]Lai, G., J. Wu, H. Ju, and F. Yan. Streptavidin-functionalized silver-nanoparticle-enriched carbon nanotube tag for ultrasensitive multiplexed detection of tumor markers. *Adv. Funct. Mater.* 21:2938–2943, 2011.
[45]Laurent, S., D. Forge, M. Port, A. Roch, C. Robic, L. Vander Elst, and R. N. Muller. Magnetic iron oxide nanoparticles: synthesis, stabilization, vectorization, physicochemical characterizations, and biological applications. *Chem. Rev.* 108:2064–2110, 2008.
[46]Levine, R. M., C. M. Scott, and E. Kokkoli. Peptide functionalized nanoparticles for nonviral gene delivery. *Soft Matter* 9:985–1004, 2013.
[47]Li, J. Application of microfluidic devices to proteomics research: identification of trace-level protein digests and affinity capture of target peptides. *Mol. Cell. Proteomics* 1:157–168, 2002.
[48]Liang, P., C.-J. Liu, R.-X. Zhuo, and S.-X. Cheng. Self-assembled inorganic/organic hybrid nanoparticles with multi-functionalized surfaces for active targeting drug delivery. *J. Mater. Chem. B* 1:4243, 2013.
[49]Lion, N., F. Reymond, H. H. Girault, and J. S. Rossier. Why the move to microfluidics for protein analysis? *Curr. Opin. Biotechnol.* 15:31–37, 2004.
[50]Lu, A., E. Salabas, and F. Schüth. Magnetic nanoparticles: synthesis, protection, functionalization, and application. *Chemie Int. Ed.*, 2007. http://onlinelibrary.wiley.com/doi/10.1002/anie.200602866/pdf.
[51]Luo, C., Q. Fu, H. Li, L. Xu, M. Sun, Q. Ouyang, Y. Chen, and H. Ji. PDMS microfludic device for optical detection of protein immunoassay using gold nanoparticles. *Lab Chip* 5:726–729, 2005.
[52]Malhotra, R., V. Patel, B. V. Chikkaveeraiah, B. S. Munge, S. C. Cheong, R. B. Zain, M. T. Abraham, D. K. Dey, J. S. Gutkind, and J. F. Rusling. Ultrasensitive detection of cancer biomarkers in the clinic by use of a nanostructured microfluidic array. *Anal. Chem.* 84:6249–6255, 2012.
[53]Mellors, J. S., W. A. Black, A. G. Chambers, J. A. Starkey, N. A. Lacher, and J. M. Ramsey. Hybrid capillary/microfluidic system for comprehensive online liquid chromatography-capillary electrophoresis-electrospray ionization-mass spectrometry. *Anal. Chem.* 85:4100–4106, 2013.
[54]Mostert, B., S. Sleijfer, J. A. Foekens, and J. W. Gratama. Circulating tumor cells (CTCs): detection methods and their clinical relevance in breast cancer. *Cancer Treat. Rev.* 35:463–474, 2009.
[55]Mucic, R. C., J. J. Storhoff, C. A. Mirkin, and R. L. Letsinger. DNA-directed synthesis of binary nanoparticle network materials. *J. Am. Chem. Soc.* 120:12674–12675, 1998.
[56]Nagrath, S., L. V. Sequist, S. Maheswaran, D. W. Bell, D. Irimia, L. Ulkus, M. R. Smith, E. L. Kwak, S. Digumarthy, A. Muzikansky, P. Ryan, U. J. Balis, R. G. Tompkins, D. A. Haber, and M. Toner. Isolation of rare circulating tumour cells in cancer patients by microchip technology. *Nature* 450:1235–1239, 2007.
[57]Ng, E., A. Gopal, K. Hoshino, and X. Zhang. Multicolor microcontact printing of proteins on nanoporous surface for patterned immunoassay. *Appl. Nanosci.* 1:79–85, 2011.
[58]Ng, E., K. Hoshino, and X. Zhang. Microfluidic immunodetection of cancer cells via site-specific microcontact printing of antibodies on nanoporous surface. *Methods* 63:266–275, 2013.
[59]Pumera, M., J. Wang, E. Grushka, and R. Polsky. Gold nanoparticle-enhanced microchip capillary electrophoresis. *Anal. Chem.* 73:5625–5628, 2001.
[60]Punnoose, E. A., S. K. Atwal, J. M. Spoerke, H. Savage, A. Pandita, R.-F. Yeh, A. Pirzkall, B. M. Fine, L. C. Amler, D. S. Chen, and M. R. Lackner. Molecular biomarker analyses using circulating tumor cells. *PLoS One* 5:e12517, 2010.
[61]Rabilloud, T. Two-dimensional gel electrophoresis in proteomics: old, old fashioned, but it still climbs up the mountains. *Proteomics* 2:3–10, 2002.
[62]Sackmann, E. K., A. L. Fulton, and D. J. Beebe. The present and future role of microfluidics in biomedical research. *Nature* 507:181–189, 2014.
[63]Sharma, T., Y. Hu, M. Stoller, M. Feldman, R. S. Ruoff, M. Ferrari, and X. Zhang. Mesoporous silica as a membrane for ultra-thin implantable direct glucose fuel cells. *Lab Chip* 11:2460–2465, 2011.
[64]Shi, J., A. P. Fang, L. Malaquin, A. Pépin, D. Decanini, J. L. Viovy, and Y. Chen. Highly parallel mix-and-match fabrication of nanopillar arrays integrated in microfluidic channels for long DNA molecule separation. *Appl. Phys. Lett.* 91:153114, 2007.
[65]Shih, S. C. C., H. Yang, M. J. Jebrail, R. Fobel, N. McIntosh, O. Y. Al-Dirbashi, P. Chakraborty, and A. R. Wheeler. Dried blood spot analysis by digital microfluidics coupled to nanoelectrospray ionization mass spectrometry. *Anal. Chem.* 84:3731–3738, 2012.
[66]Shintaku, H., H. Nishikii, L. A. Marshall, H. Kotera, and J. G. Santiago. On-chip separation and analysis of RNA and DNA from single cells. *Anal. Chem.* 86:1953–1957, 2014.
[67]Somasundaran, P. Encyclopedia of Surface and Colloid Science, Volume 1. CRC Press, 2006, https://books.google.com/books?hl=en&lr=&id=9jAHFOqyX5YC&pgis=1.

[68]Squires, T., and S. Quake. Microfluidics: fluid physics at the nanoliter scale. *Rev. Mod. Phys.* 77:977–1026, 2005.
[69]Stott, S. L., C.-H. Hsu, D. I. Tsukrov, M. Yu, D. T. Miyamoto, B. A. Waltman, S. M. Rothenberg, A. M. Shah, M. E. Smas, G. K. Korir, F. P. Floyd, A. J. Gilman, J. B. Lord, D. Winokur, S. Springer, D. Irimia, S. Nagrath, L. V. Sequist, R. J. Lee, K. J. Isselbacher, S. Maheswaran, D. A. Haber, and M. Toner. Isolation of circulating tumor cells using a microvortex-generating herringbone-chip. *Proc. Natl. Acad. Sci. USA* 107:18392–18397, 2010.
[70]Striemer, C. C., T. R. Gaborski, J. L. McGrath, and P. M. Fauchet. Charge- and size-based separation of macromolecules using ultrathin silicon membranes. *Nature* 445:749–753, 2007.
[71]Strohmeier, O., A. Emperle, G. Roth, D. Mark, R. Zengerle, and F. von Stetten. Centrifugal gas-phase transition magnetophoresis (GTM)–a generic method for automation of magnetic bead based assays on the centrifugal microfluidic platform and application to DNA purification. *Lab Chip* 13:146–155, 2013.
[72]Sun, W., C. Jia, T. Huang, W. Sheng, G. Li, H. Zhang, F. Jing, Q. Jin, J. Zhao, G. Li, and Z. Zhang. High-performance size-based microdevice for the detection of circulating tumor cells from peripheral blood in rectal cancer patients. *PLoS One* 8:e75865, 2013.
[73]Taton, T. A. Scanometric DNA array detection with nanoparticle probes. *Science* 289:1757–1760, 2000.
[74]Taylor, D. D., W. Zacharias, and C. Gercel-Taylor. Exosome isolation for proteomic analyses and RNA profiling. *Methods Mol. Biol.* 728:235–246, 2011.
[75]Théry, C., L. Zitvogel, and S. Amigorena. Exosomes: composition, biogenesis and function. *Nat. Rev. Immunol.* 2:569–579, 2002.
[76]Tiwari, J. N., R. N. Tiwari, and K. S. Kim. Zero-dimensional, one-dimensional, two-dimensional and three-dimensional nanostructured materials for advanced electrochemical energy devices. *Prog. Mater. Sci.* 57:724–803, 2012.
[77]Tsai, C.-P., C.-Y. Chen, Y. Hung, F.-H. Chang, and C.-Y. Mou. Monoclonal antibody-functionalized mesoporous silica nanoparticles (MSN) for selective targeting breast cancer cells. *J. Mater. Chem.* 19:5737, 2009.
[78]Wainright, A., U. T. Nguyen, T. Bjornson, and T. D. Boone. Preconcentration and separation of double-stranded DNA fragments by electrophoresis in plastic microfluidic devices. *Electrophoresis* 24:3784–3792, 2003.
[79]Wang, Z., H. Wu, D. Fine, J. Schmulen, Y. Hu, B. Godin, J. X. J. Zhang, and X. Liu. Ciliated micropillars for the microfluidic-based isolation of nanoscale lipid vesicles. *Lab Chip* 13:2879–2882, 2013.
[80]Whitesides, G. M. The origins and the future of microfluidics. *Nature* 442:368–373, 2006.
[81]Wilbur, J. L., A. Kumar, H. A. Biebuyck, E. Kim, and G. M. Whitesides. Microcontact printing of self-assembled monolayers: applications in microfabrication. *Nanotechnology* 7:452–457, 1996.
[82]Wu, C.-H., Y.-Y. Huang, P. Chen, K. Hoshino, H. Liu, E. P. Frenkel, J. X. J. Zhang, and K. V. Sokolov. Versatile immunomagnetic nanocarrier platform for capturing cancer cells. *ACS Nano* 7:8816–8823, 2013.
[83]Xia, H., X. Gao, G. Gu, Z. Liu, N. Zeng, Q. Hu, Q. Song, L. Yao, Z. Pang, X. Jiang, J. Chen, and H. Chen. Low molecular weight protamine-functionalized nanoparticles for drug delivery to the brain after intranasal administration. *Biomaterials* 32:9888–9898, 2011.
[84]Xia, N., T. P. Hunt, B. T. Mayers, E. Alsberg, G. M. Whitesides, R. M. Westervelt, and D. E. Ingber. Combined microfluidic-micromagnetic separation of living cells in continuous flow. *Biomed. Microdevices* 8:299–308, 2006.
[85]Xu, H., Z. P. Aguilar, L. Yang, M. Kuang, H. Duan, Y. Xiong, H. Wei, and A. Wang. Antibody conjugated magnetic iron oxide nanoparticles for cancer cell separation in fresh whole blood. *Biomaterials* 32:9758–9765, 2011.
[86]Yamada, M., K. Kano, Y. Tsuda, J. Kobayashi, M. Yamato, M. Seki, and T. Okano. Microfluidic devices for size-dependent separation of liver cells. *Biomed. Microdevices* 9:637–645, 2007.
[87]Yamada, M., and M. Seki. Hydrodynamic filtration for on-chip particle concentration and classification utilizing microfluidics. *Lab Chip* 5:1233–1239, 2005.
[88]Yang, W., Y. Cheng, T. Xu, X. Wang, and L.-P. Wen. Targeting cancer cells with biotin-dendrimer conjugates. *Eur. J. Med. Chem.* 44:862–868, 2009.
[89]Yasui, T., N. Kaji, M. R. Mohamadi, Y. Okamoto, M. Tokeshi, Y. Horiike, and Y. Baba. Electroosmotic flow in microchannels with nanostructures. *ACS Nano* 5:7775–7780, 2011.
[90]Yasui, T., N. Kaji, R. Ogawa, S. Hashioka, M. Tokeshi, Y. Horiike, and Y. Baba. Arrangement of a nanostructure array to control equilibrium and non-equilibrium transports of macromolecules. *Nano Lett.* 2015. doi:10.1021/acs.nanolett.5b00783.